ENVIRONMENTAL RESEARCH
LETTERS

LETTER • OPEN ACCESS

Recent shift from energy- to moisture-limitation over global croplands

To cite this article: Ethan D Coffel and Corey Lesk 2024 *Environ. Res. Lett.* **19** 064065

ENVIRONMENTAL RESEARCH
LETTERS

OPEN ACCESS

RECEIVED
9 June 2023

REVISED
13 May 2024

ACCEPTED FOR PUBLICATION
24 May 2024

PUBLISHED
4 June 2024

LETTER

Recent shift from energy- to moisture-limitation over global croplands

Ethan D Coffel[1,*] and Corey Lesk[2,3]

[1] Department of Geography and the Environment, Syracuse University, Syracuse, NY, United States of America
[2] Department of Geography, Dartmouth College, Hanover, NH, United States of America
[3] Neukom Institute, Dartmouth College, Hanover, NH, United States of America
[*] Author to whom any correspondence should be addressed.

E-mail: edcoffel@maxwell.syr.edu

Keywords: climate change, agriculture, climate impacts, land–atmosphere coupling, heat extremes

Supplementary material for this article is available online

Abstract

Hot and dry conditions pose a substantial risk to global crops. The frequency of co-occurring heat and drought depends on land–atmosphere coupling, which can be quantified by the correlation between temperature and evapotranspiration ($r(T, ET)$). We find that the majority of global croplands have experienced declines in $r(T, ET)$ over the past ~40 years, indicating a shift to a more moisture-limited state. In some regions, especially Europe, the sign of $r(T, ET)$ has flipped from positive to negative, indicating a transition from energy-limitation to moisture-limitation and suggesting a qualitative shift in the local climate regime. We associate stronger declines in $r(T, ET)$ with faster increases in annual maximum temperatures and larger declines in soil moisture and ET during hot days. Our results suggest that shifts towards stronger land–atmosphere coupling have already increased the sensitivity of crop yields to temperature in much of the world by 12%–37%, as hot days are not only hotter, but also more likely to be concurrently dry.

1. Introduction

Crop yields have rapidly increased since the mid-20th century due to improvements in agricultural technology, fertilizer, pest control, irrigation, and in some places, favorable climate conditions (Pingali 2012, Mueller *et al* 2016, 2017, Butler *et al* 2018, Coffel *et al* 2022b). However, many studies project large declines in crop yields in a warmer climate (Schlenker and Roberts 2009). While global yields are still rising, since 1980 rates of growth in agricultural productivity (in terms of yield and total factor productivity) has been declining in much of the world, a trend that has been partly attributed to climate change (Ray *et al* 2012, 2019, Ortiz-Bobea *et al* 2021).

Hot and dry conditions are particularly harmful for maize, soy, and wheat (Matiu *et al* 2017, Coffel *et al* 2019, Rigden *et al* 2020, Hamed *et al* 2021, Lesk *et al* 2022, Heino *et al* 2023). The extent to which hot and dry conditions co-occur is partially determined by land–atmosphere feedbacks which may be changing in magnitude as the world warms (Fischer *et al* 2007, Coffel *et al* 2019, Kornhuber *et al* 2020). The correlation between daily maximum temperature and evapotranspiration (ET) (referred to as $r(T, ET)$) can be used to measure land–atmosphere coupling and to classify locations as either moisture- or energy-limited (Seneviratne *et al* 2006, 2010, Lesk *et al* 2021, 2022, Denissen *et al* 2022). If $r(T, ET) < 0$, an increase in temperature results in a decrease in ET, suggesting that soil moisture is low and vegetation is water stressed. In these conditions, when soil moisture rises, ET rises (supplementary figure 1). In contrast, if $r(T, ET) > 0$, an increase in temperature results in an increase in ET, suggesting that there is sufficient water available for vegetation to increase transpiration in response to an increased vapor pressure deficit. In these energy-limited conditions, when surface short wave radiation (energy input) rises, ET rises (supplemental figure 2).

Previous studies have highlighted the predictive nature of $r(T, ET)$ for local crop yield sensitivity to temperature, with lower or more negative values of $r(T, ET)$ indicating greater crop yield declines in response to hot temperatures (Lesk *et al* 2021). However, little is known about whether $r(T, ET)$

has changed over global croplands during the recent decades of rapid warming, and how such changes may affect heat-drought co-occurrence and crop yield sensitivities to higher temperatures. Here, we provide evidence of a shift towards moisture-limitation over global maize, soy, and wheat growing regions over the past four decades. This shift has resulted in an increase in the strength of land–atmosphere coupling, raising the risk of concurrent heat and moisture shortage and increasing the apparent sensitivity of maize, soy, and wheat to high temperatures. The shift towards more moisture-limited conditions affects a substantial fraction of global food production, highlighting the potential impact of climate change on food security.

2. Data and methods

2.1. Calculating seasonal-scale r(T, ET)

We extract monthly mean daily maximum temperature (Tx) data from ERA5 (Hersbach *et al* 2020) and monthly mean ET data from ERA5-Land (Muñoz-Sabater *et al* 2021) over the period 1961–2021. ERA5-Land uses time-invariant maps of land cover types to estimate roughness height, albedo, and water and energy fluxes, but there is no direct representation of agriculture. However, the effects of crop growth will be reflected in the atmospheric parameters assimilated into the reanalysis, including temperature, humidity, and surface fluxes (Rodell *et al* 2004, Muñoz-Sabater *et al* 2021, Coffel *et al* 2022a).

We use time-invariant crop calendars provided by (Sacks *et al* 2010) to select Tx and ET data for months during the local maize, soy, and wheat growing seasons for each global grid cell. We linearly detrend the Tx and ET data and then we calculate $r(T, ET)$ for each grid cell as:

$$r(T,ET) = \text{corr}(\text{detrended mean growing season Tx, detrended mean growing season ET}).$$

We calculate changes in $r(T, ET)$ as:

$$\Delta r(T,ET) = r(T,ET)_{\text{period-2}} - r(T,ET)_{\text{period-1}}.$$

We calculate $r(T, ET)$ for the maize, soy, and wheat growing seasons over the time periods 1961–1980, 1971–1990, 1981–2000, 1991–2010, and 2001–2021. To assess the significance of changes in $r(T, ET)$, we upscale our grid cell-level $\Delta r(T, ET)$ map into 5×5 grid cell boxes. For each box of 25 grid cells, we use a t-test to assess the significance of the change in the mean $r(T, ET)$ between 1981–2000 and 2001–2021.

We classify $r(T, ET)$ transitions between each time period at each global grid cell into one of four groups: (1) $r(T, ET) > 0$ in both time periods; (2) $r(T, ET) < 0$ in both time periods; (3) $r(T, ET) > 0$ in time period 1 and $r(T, ET) < 0$ in time period 2; and (4) $r(T, ET) < 0$ in time period 1 and $r(T, ET) > 0$ in time period 2. For each time period, we calculate the fraction of global grid cells falling into each $r(T, ET)$ transition group.

2.2. Relating seasonal-scale r(T, ET) changes to changes in daily-scale temperature, soil moisture, and ET

We relate changes in $r(T, ET)$ to changes in local climate conditions, restricting our analysis to global grid cells between 60°S and 60°N. For each grid cell, we find the single hottest Tx value during the maize, wheat, and soy growing seasons—denoted TXx—for each grid cell in each year between 1981 and 2021. To assess changes in growing season TXx, we calculate the average growing season TXx in 1981–2000 and in 2001–2021, again considering each crop's growing season separately. We also identify the mean daily soil moisture and ET on the day of the growing season TXx for each grid cell, year, and crop, and similarly calculate averages over 1981–2000 and 2001–2021. We use the soil layers 1 and 2 in ERA5-Land, representing the first 28 cm of soil. We convert mean daily soil moisture and ET to percentile values relative to the local 1981–2021 climatology.

We use a global map of crop area from 2005 (Ramankutty *et al* 2008) to group grid cells into crop fraction deciles, ranging from 0% to 100% crop cover. For each crop fraction decile, we calculate the average $r(T, ET)$ over 1961–2021 and the average change in $r(T, ET)$ between 1981–2000 and 2001–2021.

We relate changes in $r(T, ET)$ to changes in the growing season maximum temperature (TXx), as well as to changes in soil moisture and ET occurring on the same day as the growing season maximum temperature. Our use of these metrics captures the concurrently hot and dry events that most strongly impact crop yields, enabling us to link trends in land–atmosphere coupling regimes to observed crop impacts (Lobell *et al* 2013, Coffel *et al* 2019, 2019, Schlenker and Roberts 2009). We conduct this analysis for all cropped grid cells and for bins of grid cells grouped by crop fraction. We group grid cells with crop fractions between 0%–1%, 1%–2%, to 99%–100%, for a total of 100 bins. For all grid cells in each crop fraction bin, we calculate the average change in growing season TXx, and soil moisture and ET values on the growing season TXx days over the 1981–2000 and 2001–2021 periods. We then use ordinary least squares regression to associate the average $r(T, ET)$ change in each crop fraction bin to the average change in growing season TXx, soil moisture, and ET on the TXx day. This analysis is conducted separately for each crop's growing season.

2.3. Calculating the sensitivity of maize, soy, and wheat yields to growing season mean Tx at each global grid cell

We calculate crop yield sensitivity to growing season mean temperature using the following procedure:

1. We calculate a crop-specific mean Tx during the local growing season for maize, soy, and wheat, using a crop calendar from (Sacks *et al* 2010). We exclude all grid cells with zero crop fraction for the selected crop, and we restrict our data to 1981–2016, matching the availability of global yield data.
2. For each grid cell, we linearly detrend maize, soy, and wheat yield data from (Iizumi and Sakai 2020) covering 1981–2016. Linear detrending is commonly used to remove the long-term technology-driven yield trend, allowing for analysis of the climate-driven yield anomalies. However, for some regions and some time periods, trends in agricultural yields may be non-linear. We account for this by repeating this analysis and detrending via non-parametric singular spectrum analysis, which does not assume a functional form for the yield trend. Results using this alternate detrending methodology are presented in supplementary figures 3 and 4.
3. We linearly detrend our crop-specific mean growing season Tx time series for each grid cell.
4. We standardize temperature and yield anomalies by dividing the detrended anomalies by their standard deviation for each grid cell.
5. We calculate crop yield sensitivity as the ordinary least squares regression slope between detrended growing season mean Tx and detrended yield anomalies. We label this yield sensitivity $Y_{\text{sensitivity},x,y,c}$, where the $_c$ represents each of our three crops: maize, soy, and wheat, and the $_{x,y}$ represents each grid cell.

2.4. Relating crop yield sensitivity to r(T, ET) across grid cells and estimate the changes in yield sensitivity associated with changes in r(T, ET)

We then regress grid cell-specific crop yield sensitivity against mean growing season $r(T, ET)$ between 1981–2016, giving us $\frac{\Delta Y_{\text{sensitivity},x,y,c}}{\Delta r(T,ET)}$ for maize, soy, and wheat. To assess how changes in $r(T, ET)$ have influenced yield sensitivity to mean Tx, we first calculate the difference in $r(T, ET)$ between the periods 2001–2021 and 1981–2000 for all grid cells with non-zero crop fractions for each crop. We then calculate the change in yield sensitivity for each crop as:

$$\Delta Y_{\text{sensitivity},x,y,c} = \frac{\Delta Y_{\text{sensitivity},x,y,c}}{\Delta r(T,ET)} * \Delta r(T,ET)_{x,y,c}.$$

We calculate percent changes in global $\Delta Y_{\text{sensitivity},c}$ as the change in the 50th percentile value across grid cells. We also calculate how changes in yield sensitivity to temperature affect production sensitivity to temperature as:

$$\Delta P_{x,y,c} = \overline{Y_{x,y,c}} * A_{x,y,c} * \Delta Y_{\text{sensitivity},x,y,c}$$

where $\Delta P_{x,y,c}$ is the change in production per degree C at a given grid cell and for a specific crop, $\overline{Y_{x,y,c}}$ is the mean yield from 1981 to 2016 for the crop and grid cell, $A_{x,y,c}$ is the harvested area for the crop and grid cell, and $\Delta Y_{\text{sensitivity},x,y,c}$ is the change in yield sensitivity for the crop and grid cell associated with changes in $r(T, ET)$. The percentage change in production per degree C is calculated as the sum of $\Delta P_{x,y,c}$ for each grid cell divided by the sum of total global production for that crop.

3. Results and discussion

A majority of global croplands are concentrated in moisture limited regions ($r(T, ET) < 0$), and higher crop fractions are associated with more moisture limitation (figures 1(a), (c) and supplementary figure 5(d)). We do not find evidence that $r(T, ET)$ itself is strongly influenced by the ET produced by crop growth; rather, it is determined by large-scale climate dynamics and regional land–atmosphere interaction (supplemental table 1). There is substantial variability in $r(T, ET)$ over croplands, with some breadbasket regions, such as northern Europe, being largely energy-limited ($r(T, ET) > 0$) over the period 1961–2021. Since 1961, mean $r(T, ET)$ has declined over 61% of global croplands, with 44% and 30% experiencing declines of more than −0.1 and −0.2, respectively (figure 1(e)). Such negative changes in $r(T, ET)$ indicate shifts towards greater moisture-limitation, and have occurred over both low- and high-intensity cropland (figures 1(b) and (d)). The majority of these declines in $r(T, ET)$ occurred between the time periods of 1981–2000 and 2001–2021, a time period coinciding with rapid global warming. Between 1961–1980 and 1981–2000, $r(T, ET)$ declined but by a smaller amount in most cropped regions. Declines in $r(T, ET)$ between 1961–1980 and 1981–2000 are not statistically significant (t-test, $p > 0.05$) for most crop fraction bins. However, between 1981–2000 and 2001–2021, most crop fraction bins experience statistically significant declines in $r(T, ET)$ (figure 1(d)), representing the recent shift towards moisture-limitation. Declines in $r(T, ET)$ are spatially heterogeneous, with the largest declines concentrated in northern Europe, parts of South America, and central Africa (figure 1(b)). The former two of these regions of predominantly declining $r(T, ET)$ are consistent with projections under greenhouse gas forcing from Coupled Model Intercomparison Project phase 6 and earlier models (Seneviratne *et al* 2006, 2010, Lesk *et al* 2021). Regions of increasing $r(T, ET)$ are generally smaller in spatial extent and weaker in magnitude than regions of declining $r(T, ET)$. Globally, we find that between 1981–2000 and 2001–2021, 61% of cropped land experienced declines in $r(T, ET)$ and only 39% of cropped land experienced increases.

The decline in growing season $r(T, ET)$ has resulted in some areas switching from energy-limitation ($r(T, ET) > 0$) to moisture-limitation ($r(T, ET) < 0$),

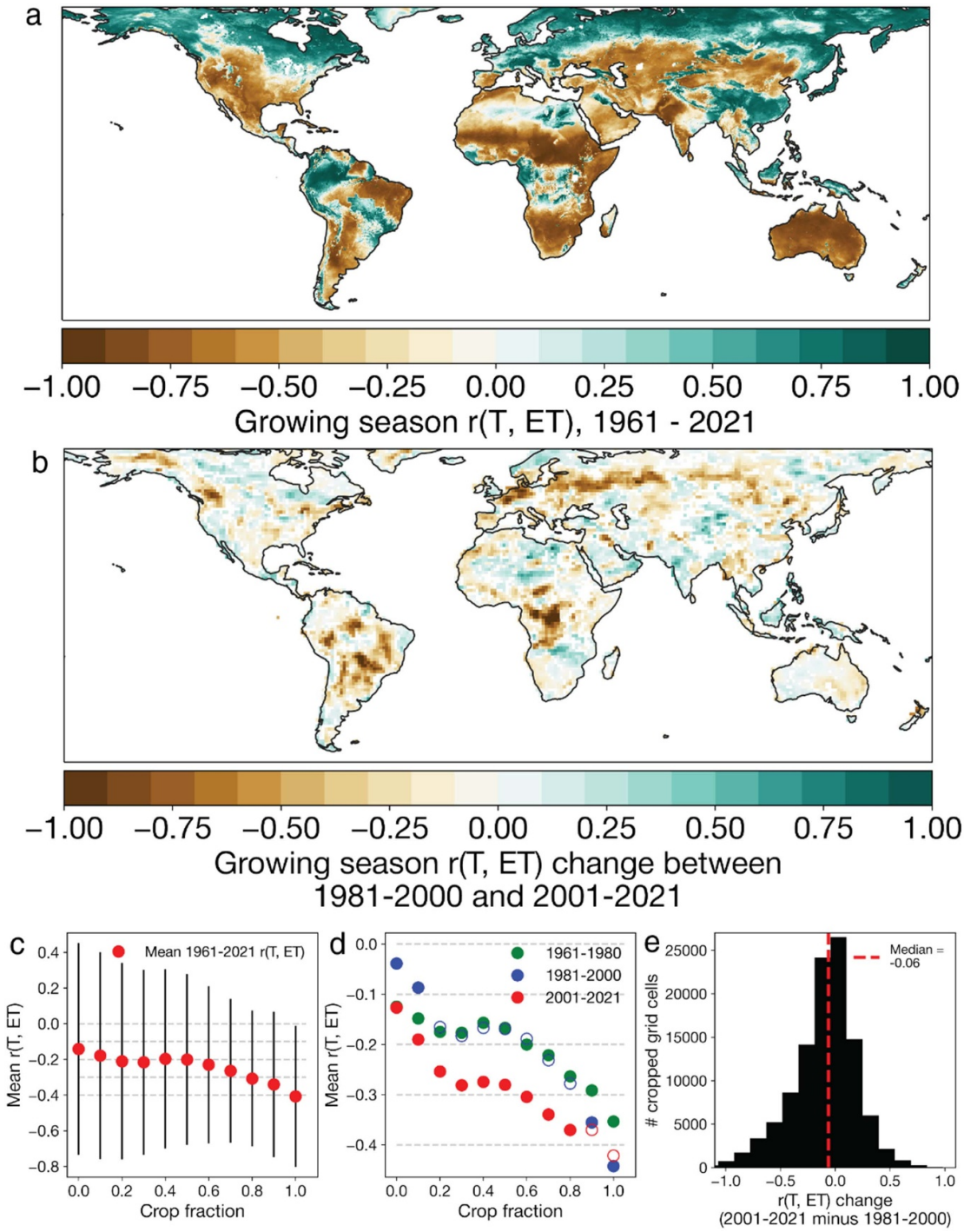

Figure 1. Correlation between growing season average daily maximum temperature and growing season average evapotranspiration ($r(T, ET)$). (a) Historical $r(T, ET)$ averaged over maize growing seasons between 1961 and 2021. (b) Change in growing season $r(T, ET)$ between 1981–2000 and 2001–2021 with only significant ($p < 0.05$, t-test) changes shown. (c) Historical $r(T, ET)$ averaged over the maize growing season between 1961 and 2021 for all grid cells in crop fraction deciles (0% crop cover to 100% crop cover). Black vertical lines show the 25th–75th percentile range across grid cells in each bin. (d) Historical $r(T, ET)$ averaged over maize growing seasons between 1961–2021 and averaged over all grid cells in crop fraction deciles in three time periods: 1961–1980 (green), 1981–2000 (blue), and 2001–2021 (red). Solid blue and red markers indicate that the $r(T, ET)$ mean is significantly (t-test, $p < 0.05$) different from the preceding period (2001–2021 different from 1981–2000, and 1981–2000 different from 1961 to 1980). (e) Distribution of $r(T, ET)$ changes between 1981–2000 and 2001–2021 across all cropped grid cells.

indicating a fundamental shift in a region's land–atmosphere coupling regime. To identify potential regime changes, we track categorical shifts in $r(T, ET)$ over three time periods: 1961–1980–1981–2000, 1971–1990–1991–2010, and 1981–2000–2001–2021. The shift from energy- to moisture-limitation since 1961 has been extensive in Northern and Eastern Europe, central Russia, and eastern India, with more localized shifts in parts of the central US northeastern China, parts of Argentina and Brazil, and central Africa (figures 2(a), (c), (e) and supplementary figure 5). Notably, we detect such regime shifts in

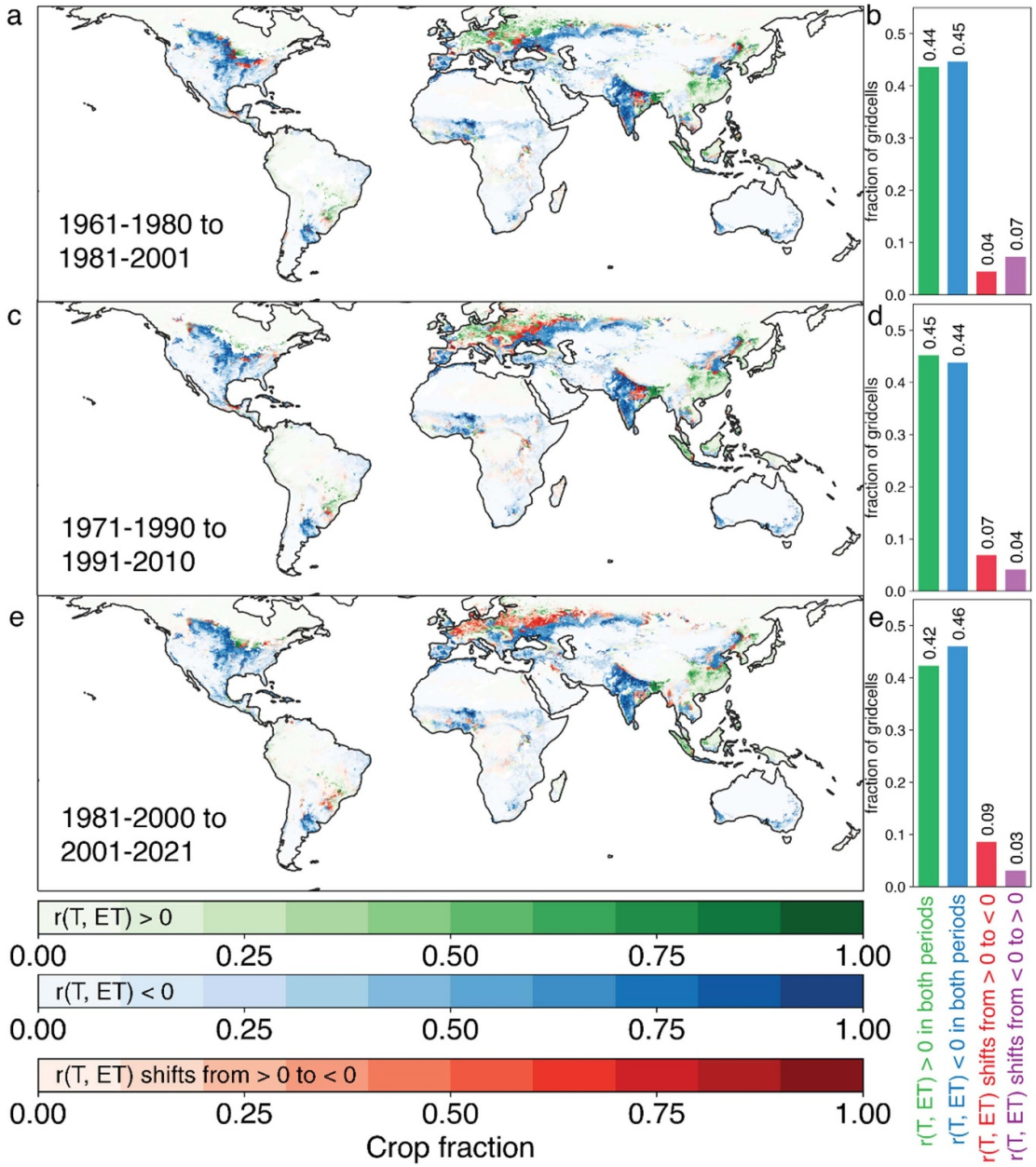

Figure 2. Change in $r(T, ET)$ during the maize growing season. (a), (c), (e) Historical $r(T, ET)$ changes between (a) 1961–1980 and 1981–2000; (c) 1971–1990 and 1991–2010; and (e) 1981–2000 and 2001–2021. Green colors show grid cells where $r(T, ET)$ is greater than zero in both time periods, blue colors show grid cells where $r(T, ET)$ is less than zero in both time periods, and red colors show grid cells where $r(T, ET)$ is greater than zero in the first time period and less than zero in the second time period. Color intensity represents grid cell crop fraction. (b), (d), (e) Fraction of global cropped grid cells in each group (green, blue, red) in each time period, as well as the fraction of grid cells with $r(T, ET)$ less than zero in the first period and greater than zero in the second period (purple).

at least some portion of nearly all major crop producing regions of the globe. The amount of global land transitioning from energy- to moisture limitation has increased from 4% to 7% to 9% over our three time periods, respectively (figures 2(b), (d) and (e)). At the same time, the amount of global land transitioning from moisture- to energy-limitation has declined from 7% to 4% to 3%. Between the three time periods, 1.2% of global grid cells flipped from energy-limitation to moisture-limitation and back to energy-limitation, and another 3.9% of global grid cells flipped from moisture-limitation to energy-limitation and back to moisture-limitation, indicating that we are mostly seeing a steady shift towards moisture-limitation, with fluctuations being less widespread. Much of the world's croplands were in moisture-limited regions in all time periods: these areas experienced mean $r(T, ET)$ declines of 0.04 between 1981–2000 and 2001–2021.

Decreases in seasonal-scale $r(T, ET)$ are associated with increases in the magnitude of daily-scale hot and dry conditions, as measured by growing season maximum temperatures (TXx) and in soil moisture and ET on the TXx day (figures 3(a), (d) and

(g)). These hot days are disproportionately important to global agriculture, as concurrent hot and dry conditions drive substantial yield losses (Schlenker and Roberts 2009, Lobell *et al* 2013, Coffel *et al* 2019, Lesk *et al* 2022). Across global cropland, a unit decline in $r(T, ET)$ is associated with an increase in TXx of 0.67 °C, and a 5.7 percentage point decline in both soil moisture and ET on the TXx day. While these relationships are significant ($p < 0.01$) and relatively large in magnitude, $r(T, ET)$ explains only a small fraction of the spatial variability in TXx, soil moisture, and ET change, with R^2 values of 0.1, 0.07, and 0.03, respectively; the low R^2 values indicate the influence of atmospheric dynamics, land use, and other factors that drive local climate change. Change in ET has a weaker relationship with $r(T, ET)$ change than temperature or soil moisture, potentially due to the influence of strong trends in crop production on local ET in some major breadbasket regions (Coffel *et al* 2022a, 2022b).

Because high-production cropped regions are spatially concentrated, we bin our results by crop fraction to show how $r(T, ET)$, TXx, and soil moisture and ET on the TXx day change across different levels of cropping intensities. Binning grid cells by crop fraction (100 bins, crop fractions 0%–100%) substantially strengthens the relationship between $r(T, ET)$ and local climate variables (figures 3(b), (e) and (h)). Across crop fraction bins, those with more negative changes in $r(T, ET)$ see larger increases in TXx: a decline in $r(T, ET)$ of −0.1 is associated with an increase in growing season TXx of about 0.6 °C, while no change in $r(T, ET)$ is associated with an increase in growing season TXx of about 0.3 °C (figure 3(b)). These results suggest that the magnitude of the declines in $r(T, ET)$ that occur over many croplands are associated with an approximate doubling of the rate of TXx warming as compared to places with no change in $r(T, ET)$.

Grid cells where $r(T, ET)$ shifts from positive (energy-limitation) to negative (moisture-limitation) have the largest increases in TXx (figure 3(c)), and places where $r(T, ET)$ shifts from negative to positive have the smallest increases in TXx. These tendencies are mirrored for soil moisture and ET: larger declines in $r(T, ET)$ are associated with larger declines in soil moisture and ET on the TXx day (figures 3(f) and (i)), and the largest declines in soil moisture on TXx days are found where $r(T, ET)$ shifts from positive to negative (figure 3(f)). In these grid cells that transition from energy- to moisture-limitation, the mean TXx change is 0.9 °C (range from 0.6 °C to 1.2 °C), and the mean soil moisture and ET percentile changes on the TXx days are −6 and −4 percentage points, respectively (with ranges from −9 to −3 and from −7 to 0 percentage points, respectively). These relationships are similar for maize, soy, and wheat (supplementary figure 6), and suggest that negative $r(T, ET)$ shifts correspond to increasing concurrent crop stresses.

Across crop fraction bins, changes in $r(T, ET)$ loosely cluster into two broad buckets: regions with small changes (−0.05 to 0.05) and regions with substantial declines (around −0.1, figures 2(a), (c) and (e)). Global regions with similar crop fractions are spatially grouped, especially for the most intensely cropped areas like the US Midwest, eastern Europe, northeast China, much of India, parts of West Africa, and southeast South America (supplementary figure 5(d)). Regions with very high crop fractions (>0.8) generally fall in the former bucket, undergoing smaller and non-significant $r(T, ET)$ changes in the 1981–2000–2001–2021 period. However, these high crop fraction regions experienced earlier declines in $r(T, ET)$ between 1961–1980 and 1981–2000 (figure 1(d)). More recent changes in $r(T, ET)$ in these densely cropped bins may have partly been limited by the crop-driven cooling induced by strong yield improvements in some areas (Mueller *et al* 2016, 2017, Butler *et al* 2018, Coffel *et al* 2022b). While recent trends in $r(T, ET)$ may have relatively spared the most densely cropped regions, the persistence of negative $r(T, ET)$ shifts in small portions of densely cropped regions signals the potential for more widespread change under continued warming (DeLucia *et al* 2019).

The more substantial declines in $r(T, ET)$ have occurred in low and moderate crop fraction regions. Since 1981, Northern Europe and Russia have had among the largest and most widespread $r(T, ET)$ declines, and are also breadbasket regions with crop fractions commonly between 0.4 and 0.8. Northern Europe is also the region with the most pronounced shift from energy- to moisture-limitation (figures 2(a), (c) and (e)), and associated increases in TXx and declines in soil moisture and ET on TXx days (figure 3).

Lower $r(T, ET)$ values are associated with higher yield sensitivity to growing season mean Tx since 1981 for maize, soy, and wheat (figures 4(a)–(c)): in regions with lower $r(T, ET)$ values, crops lose more yield per degree increase in temperature. We find no relationship between annual mean temperature and yield sensitivity (supplementary figure 7). The strength of the association between $r(T, ET)$ and yield sensitivity to temperature varies between crops, with an R^2 value of 0.23 for maize, 0.45 for soy, and 0.11 for wheat. Like previous studies, we find that soy yield sensitivity to temperature is more strongly associated with $r(T, ET)$ than for maize or wheat (Hamed *et al* 2021, Lesk *et al* 2021, Proctor *et al* 2022). Globally, 67% of croplands have negative $r(T, ET)$ between 1961 and 2021. Consistent with this broad moisture limitation, most maize, soy, and wheat (by area) experience declining yields with higher temperatures: about 66% of global maize, 59% of soy,

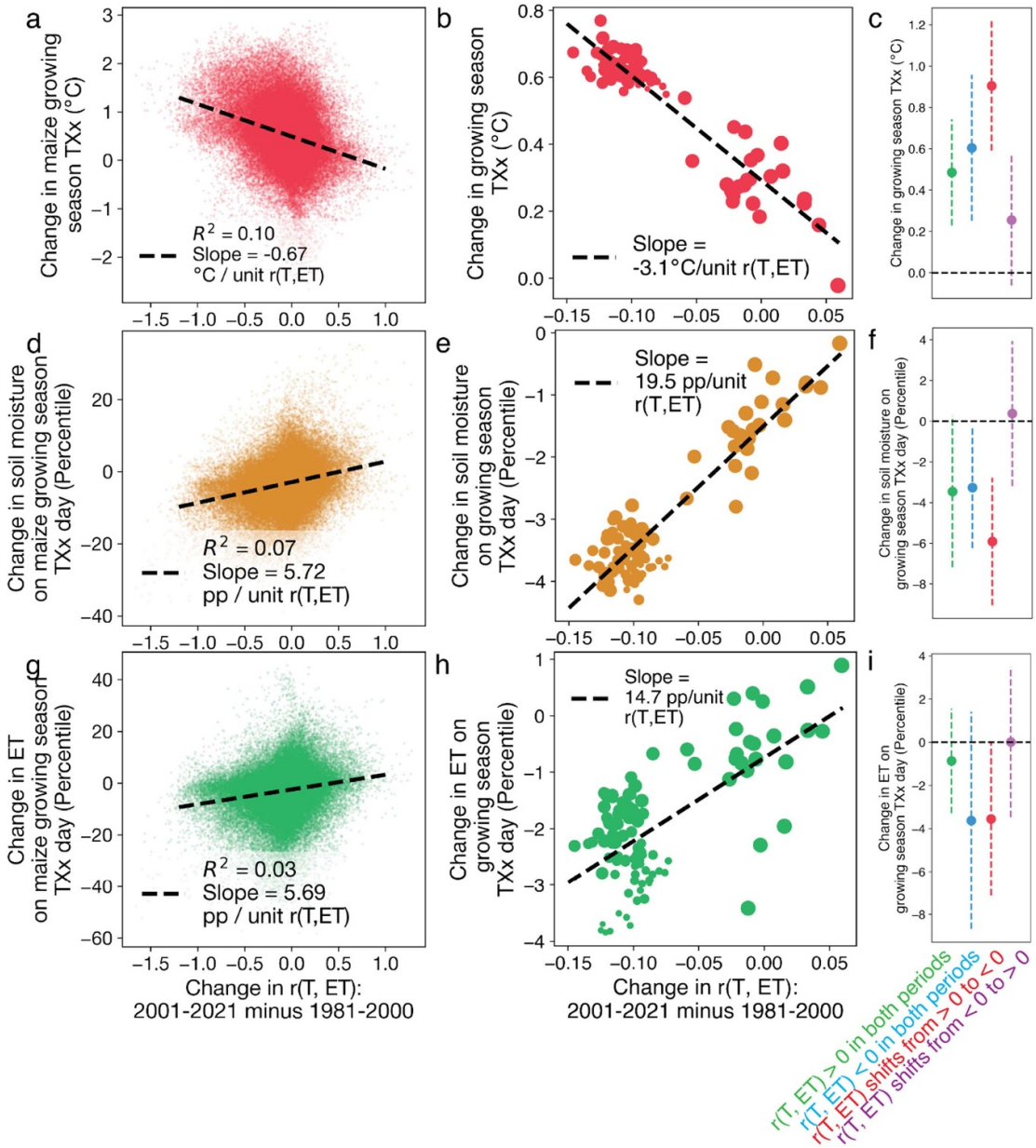

Figure 3. Relationship between changes in $r(T, ET)$ and changes in climate conditions during heat extremes over croplands between 1981–2000 and 2001–2021. (a)–(c) Change in local $r(T, ET)$ vs. change in annual maximum temperature during the maize growing season (TXx) for (a) all global grid cells with crops; (b) grid cells binned by crop fraction; (c) grid cells binned by $r(T, ET)$ shift. (d)–(f) Same as for (a)–(c) but for the soil moisture percentile on the TXx day. (g)–(i) Same as (a)–(c) but for the ET percentile on the TXx day. In (b), (e), (h) points show averages over grid cells with crop fraction percentiles between 1 and 100, with the size of the point indicating the crop fraction (larger points for higher crop fractions). Black dashed lines show an ordinary least squares regression through points. (c), (f), (i) show mean changes in growing season TXx and soil moisture and ET on the TXx day for grid cells where $r(T, ET)$ is greater than zero in both time periods (green), $r(T, ET)$ is less than zero in both time periods (blue), $r(T, ET)$ is greater than zero in the first time period and less than zero in the second (red), and $r(T, ET)$ is less than zero in the first time period and greater than zero in the second (purple). Error bars show 1 standard deviation across grid cells in each group.

and 72% of wheat crops have negative yield sensitivity to temperature, indicating that warming would likely be harmful. We use these relationships between historical $r(T, ET)$ and yield sensitivity to temperature to estimate the change in yield sensitivity that has occurred between 1981–2000 and 2001–2021 due to the observed change in $r(T, ET)$.

We find that $r(T, ET)$ has declined over maize-growing regions by 0.14 (from $r(T, ET) = -0.31$ to -0.45), over soy-growing regions by 0.10 (from $r(T, ET) = -0.14$ to -0.24), and over wheat-growing regions by 0.10 (from $r(T, ET) = -0.31$ to -0.41) (figure 4(d)). We estimate that this decline in $r(T, ET)$ has increased the standardized sensitivity of maize to growing season mean Tx (implying more yield loss per °C) by 23.2% (-0.095 to -0.124 SD/°C), soy by 36.7% (-0.063 to -0.099 SD/°C), and wheat by 12.0% (-0.144 to -0.164 SD/°C) (figure 4(e)). To assess the impact of these changes in yield sensitivity on global food supply, we estimate how the

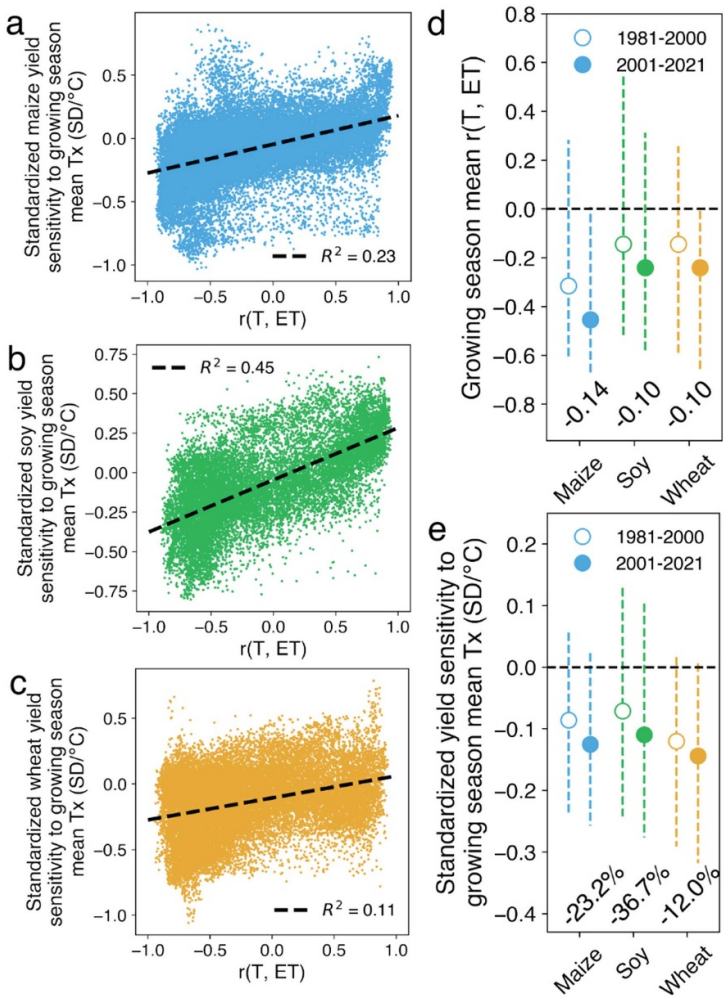

Figure 4. Relationship between $r(T, ET)$ and crop yield sensitivity to temperature. (a)–(c) Historical $r(T, ET)$ vs. yield sensitivity to growing season average Tx for maize (a), soy (b), and wheat (c) between 1981–2016. (d) Change in $r(T, ET)$ between 1981–2000 and 2001–2021 over croplands for maize, soy, and wheat. Vertical dashed lines show the 25th–75th percentile range across grid cells. (e) Yield sensitivity to growing season average Tx in 1981–2000 (open circles) and 2001–2021 (filled circles) for maize (blue), soy (green), and wheat (orange). Vertical dashed lines show the 25th–75th percentile range across grid cells. Percentages in (d), (e) show the change in the 50th percentile $r(T, ET)$ and yield sensitivity value for each crop.

sensitivity of global maize, soy, and wheat production has changed as a result of $r(T, ET)$ changes. We estimate that changes in $r(T, ET)$ globally increase the sensitivity of global maize, soy, and wheat production to growing season mean Tx by 6.1%, 23.2%, and 6.4%, respectively. Production impacts are smaller than yield impacts in fractional terms because the highest-production regions—those with high mean yields and high harvested area—have seen relatively smaller changes in $r(T, ET)$ in recent decades. Our results are robust when excluding irrigated croplands: removing all grid cells with more than 1% of crops irrigated does not substantially change our main result (supplementary figure 8). We note that other factors including agricultural management practices, changes in soil quality, and pests may also influence the sensitivity of crops to temperature; here we only examine the global change in yield sensitivity associated with $r(T, ET)$ change, irrespective of these regional factors that may modify these relationships locally.

A few limitations of our study signal priorities and nuances for future research. First, we do not directly account for the influence of rising atmospheric CO_2 on crop water-use efficiency, whose magnitude remains highly uncertain (Ainsworth and Long 2021, Taylor and Schlenker 2021). While this water-use efficiency boost may partly offset the general impact of warming on yields, it also may enable stricter stomatal regulation and reduced transpiration during high temperatures, potentially enhancing local land–atmosphere coupling. Large uncertainties on the magnitude of these effects preclude directly estimating the CO_2 fertilization effect in this study, but the trend towards increasing temperature sensitivity that we observe here has occurred in the context of rapidly rising atmospheric CO_2 levels, suggesting that the CO_2 fertilization effect is implicitly accounted for and

may play some causative role in our results. Our study underscores that future research should consider the potential for enhanced water-use efficiency to both raise yields through CO_2 fertilization as well as lower them through negative $r(T, ET)$ shifts.

Second, we use ET data from ERA5-Land, which is a model-based product and has its own biases relative to the real world, particularly in poorly observed variables like ET. However, past research has found that ERA5-Land ET data closely matches other global ET products like GLDAS (Coffel *et al* 2022a). Nevertheless, there is likely bias introduced into our results due to underlying ET biases in ERA5-Land. Third, we do not consider agricultural adaptations such as irrigation expansion (Siebert *et al* 2017, Zaveri and Lobell 2019, Rosa 2022), crop migration (Sloat *et al* 2020), and genetic modification (Pingali 2012), which are already occurring and will likely continue as climate change impacts intensify. The effects of such adaptations are relatively well understood for individual heat or drought stresses, but less so for the combination thereof. For instance, yield sensitivity to drought, perhaps attributable to rising sowing densities, may have intensified in some regions over the period examined in this study (Lobell *et al* 2014, David *et al* 2020). We find no relationship between changes in $r(T, ET)$ and changes in maize, soy, or wheat yields (supplemental figure 9). While $r(T, ET)$ changes are associated with changes in yield sensitivity to temperature, yield itself is strongly modulated by the wide variety of technological, management, and other factors that have increased crop growth and for which global observations are critically lacking. Future work should consider whether these trends are a result or even a cause of $r(T, ET)$ changes.

We find evidence for a widespread decline in $r(T, ET)$, over global croplands between 1981–2000 and 2001–2021. Such changes in land–atmosphere coupling include an outright shift from energy- to moisture-limitation over some regions, especially in Europe. This increasing moisture limitation has been associated with an enhanced warming of annual maximum temperatures and declining soil moisture and ET levels on hot days, changes which have increased the sensitivity of maize, soy, and wheat yields to growing season mean temperature. This relationship between $r(T, ET)$ and yield sensitivity to temperature, coupled with the fact that the latest generation of earth system models projects continued declines of $r(T, ET)$ across global croplands (Seneviratne *et al* 2006, 2010, Lesk *et al* 2021), suggests that the yields of staple crops may continue to become more sensitive to temperature in the future, exacerbating the effect of increasingly frequent and intense heat on agriculture. Climate models project a global transition from energy- to moisture-limitation with negative impacts on crops in a warming world, and our results suggest that this transition is already underway.

Data availability statement

Crop yield data are freely available from Pangaea at https://doi.pangaea.de/10.1594/PANGAEA.909132. ERA5 and ERA5-Land climate data are freely available from the European Center for Medium Range Forecasting. Analysis code available at https://github.com/ecoffel/2021-heat.

Conflict of interest

The authors have no conflicts of interest.

Funding

E D C is supported by NSF Awards 2049262 and 2304953. C L is supported by the Dartmouth College Neukom Institute.

ORCID iD

Ethan D Coffel https://orcid.org/0000-0003-3172-467X

References

Ainsworth E A and Long S P 2021 30 years of free-air carbon dioxide enrichment (FACE): what have we learned about future crop productivity and its potential for adaptation? *Glob. Change Biol.* **27** 27–49

Butler E E, Mueller N D and Huybers P 2018 Peculiarly pleasant weather for US maize *Proc. Natl Acad. Sci.* **115** 11935–40

Coffel E D, Horton R M, Winter J M and Mankin J S 2019 Nonlinear increases in extreme temperatures paradoxically dampen increases in extreme humid-heat *Environ. Res. Lett.* **14** 084003

Coffel E D, Keith B, Lesk C, Horton R M, Bower E, Lee J and Mankin J S 2019 Future hot and dry years worsen Nile basin water scarcity despite projected precipitation increases *Earth's Future* **7** 967–77

Coffel E D, Lesk C and Mankin J S 2022a Earth system model overestimation of cropland temperatures scales with agricultural intensity *Geophys. Res. Lett.* **49** e2021GL097135

Coffel E D, Lesk C, Winter J M, Osterberg E C and Mankin J S 2022b Crop-climate feedbacks boost US maize and soy yields *Environ. Res. Lett.* **17** 024012

DeLucia E H *et al* 2019 Are we approaching a water ceiling to maize yields in the United States? *Ecosphere* **10** e02773

Denissen J M C, Teuling A J, Pitman A J, Koirala S, Migliavacca M, Li W, Reichstein M, Winkler A J, Zhan C and Orth R 2022 Widespread shift from ecosystem energy to water limitation with climate change *Nat. Clim. Change* **12** 677–84

Fischer E M, Seneviratne S I, Lüthi D and Schär C 2007 Contribution of land-atmosphere coupling to recent European summer heat waves *Geophys. Res. Lett.* **34** L06707

Hamed R, Van Loon A F, Aerts J and Coumou D 2021 Impacts of compound hot–dry extremes on US soybean yields *Earth Syst. Dyn.* **12** 1371–91

Heino M, Kinnunen P, Anderson W, Ray D K, Puma M J, Varis O, Siebert S and Kummu M 2023 Increased probability of hot and dry weather extremes during the growing season threatens global crop yields *Sci. Rep.* **13** 3583

Hersbach H *et al* 2020 The ERA5 global reanalysis *Q. J. R. Meteorol. Soc.* **146** 1999–2049

Iizumi T and Sakai T 2020 The global dataset of historical yields for major crops 1981–2016 *Sci. Data* **7** 97

Kornhuber K, Coumou D, Vogel E, Lesk C, Donges J F, Lehmann J and Horton R M 2020 Amplified Rossby waves enhance risk of concurrent heatwaves in major breadbasket regions *Nat. Clim. Change* **10** 48–53

Lesk C, Anderson W, Rigden A, Coast O, Jägermeyr J, McDermid S, Davis K F and Konar M 2022 Compound heat and moisture extreme impacts on global crop yields under climate change *Nat. Rev. Earth Environ.* **3** 872–89

Lesk C, Coffel E, Winter J, Ray D, Zscheischler J, Seneviratne S I and Horton R 2021 Stronger temperature–moisture couplings exacerbate the impact of climate warming on global crop yields *Nat. Food* **2** 683–91

Lobell D B, Deines J M and Tommaso S D 2020 Changes in the drought sensitivity of US maize yields *Nat. Food* **1** 729–35

Lobell D B, Hammer G L, McLean G, Messina C, Roberts M J and Schlenker W 2013 The critical role of extreme heat for maize production in the United States *Nat. Clim. Change* **3** 497–501

Lobell D B, Roberts M J, Schlenker W, Braun N, Little B B, Rejesus R M and Hammer G L 2014 Greater sensitivity to drought accompanies maize yield increase in the U.S. Midwest *Science* **344** 516–9

Matiu M, Ankerst D P and Menzel A 2017 Interactions between temperature and drought in global and regional crop yield variability during 1961–2014 *PLoS One* **12** e0178339

Mueller N D, Butler E E, McKinnon K A, Rhines A, Tingley M, Holbrook N M and Huybers P 2016 Cooling of US Midwest summer temperature extremes from cropland intensification *Nat. Clim. Change* **6** 317–22

Mueller N D, Rhines A, Butler E E, Ray D K, Siebert S, Holbrook N M and Huybers P 2017 Global relationships between cropland intensification and summer temperature extremes over the last 50 years *J. Clim.* **30** 7505–28

Muñoz-Sabater J *et al* 2021 ERA5-Land: a state-of-the-art global reanalysis dataset for land applications *Earth Syst. Sci. Data* **13** 4349–83

Ortiz-Bobea A, Ault T R, Carrillo C M, Chambers R G and Lobell D B 2021 Anthropogenic climate change has slowed global agricultural productivity growth *Nat. Clim. Change* **11** 306–12

Pingali P L 2012 Green revolution: impacts, limits, and the path ahead *Proc. Natl Acad. Sci.* **109** 12302–8

Proctor J, Rigden A, Chan D and Huybers P 2022 More accurate specification of water supply shows its importance for global crop production *Nat. Food* **3** 753–63

Ramankutty N, Evan A T, Monfreda C and Foley J A 2008 Farming the planet: 1. Geographic distribution of global agricultural lands in the year 2000 *Glob. Biogeochem. Cycles* **22** GB1003

Ray D K, Ramankutty N, Mueller N D, West P C and Foley J A 2012 Recent patterns of crop yield growth and stagnation *Nat. Commun.* **3** 1293

Ray D K, West P C, Clark M, Gerber J S, Prishchepov A V and Chatterjee S 2019 Climate change has likely already affected global food production *PLoS One* **14** e0217148

Rigden A J, Mueller N D, Holbrook N M, Pillai N and Huybers P 2020 Combined influence of soil moisture and atmospheric evaporative demand is important for accurately predicting US maize yields *Nat. Food* **1** 127–33

Rodell M *et al* 2004 The global land data assimilation system *Bull. Am. Meteorol. Soc.* **85** 381–94

Rosa L 2022 Adapting agriculture to climate change via sustainable irrigation: biophysical potentials and feedbacks *Environ. Res. Lett.* **17** 063008

Sacks W J, Deryng D, Foley J A and Ramankutty N 2010 Crop planting dates: an analysis of global patterns: global crop planting dates *Glob. Ecol. Biogeogr.* **19** 607–20

Schlenker W and Roberts M J 2009 Nonlinear temperature effects indicate severe damages to U.S. crop yields under climate change *Proc. Natl Acad. Sci.* **106** 15594–8

Seneviratne S I, Corti T, Davin E L, Hirschi M, Jaeger E B, Lehner I, Orlowsky B and Teuling A J 2010 Investigating soil moisture–climate interactions in a changing climate: a review *Earth Sci. Rev.* **99** 125–61

Seneviratne S I, Lüthi D, Litschi M and Schär C 2006 Land–atmosphere coupling and climate change in Europe *Nature* **443** 205–9

Siebert S, Webber H, Zhao G and Ewert F 2017 Heat stress is overestimated in climate impact studies for irrigated agriculture *Environ. Res. Lett.* **12** 054023

Sloat L L, Davis S J, Gerber J S, Moore F C, Ray D K, West P C and Mueller N D 2020 Climate adaptation by crop migration *Nat. Commun.* **11** 1243

Taylor C and Schlenker W 2021 *Environmental Drivers of Agricultural Productivity Growth: CO_2 Fertilization of US Field Crops* (National Bureau of Economic Research) p w29320

Zaveri E and Lobell B D 2019 The role of irrigation in changing wheat yields and heat sensitivity in India *Nat. Commun.* **10** 4144